[4] W. G. Matthei and W. Crowe, "New microwave integrated circuit modules," *WESCON Tech. Papers*, vol. 12, pp. 2/1-1–2/1-6, Aug. 1968.
[5] H. C. Okean, "Microwave amplifiers employing integrated tunnel-diode devices," *IEEE Trans. Microwave Theory Tech.*, vol. MTT-15, pp. 613–622, Nov. 1967.
[6] J. D. Welch, "Beam lead tunnel-diode amplifiers on microstrip," in *1970 G-MTT Int. Symp. Dig.*, pp. 212–216, 1970.
[7] R. Steinhoff and F. Sterzer, "Microwave tunnel-diode amplifiers with large dynamic range," *RCA Rev.*, vol. 25, pp. 54–66, Mar. 1964.
[8] S. Virk, "The state of tunnel-diode technology," *Electron. Products*, pp. 30–32, Nov. 1969.
[9] A. Lueck, W. Schultz, and A. Marmiani, "The solid structure tunnel diode," *Microwave J.*, vol. 9, pp. 49–52, July 1966.
[10] H. C. Okean, "Synthesis of negative resistance reflection amplifiers employing band-limited circulator," *IEEE Trans. Microwave Theory Tech.*, vol. MTT-14, pp. 323–337, July 1966.

Correspondence

Slot-Line Field Components

SEYMOUR B. COHN

***Abstract*—Formulas derived by mode summation give the six E- and H-field components in the various air and dielectric regions of a slot-line cross section. These formulas are valid except when very close to the slot, where approximations in the analysis cause a large error. A quasi-static method yields a second set of formulas that apply near the slot. Thus the field is determined satisfactorily in all parts of the cross section. Graphs of the H components show that elliptical polarization exists, with the best approach to circularity near the slot and near the opposite surface of the substrate. Quantitative field data are useful for analysis and design of slot-line components, such as ferrite devices, dielectric-resonator filters, directional couplers, and broad-band transitions to coaxial line or microstrip.**

I. Introduction

Several earlier papers [1]–[7] show that slot line has interesting potentialities for microwave integrated circuits on dielectric substrates. The analysis of slot-line wavelength, group velocity, and characteristic impedance [1] has been extended to yield the field components as functions of frequency, slot-line constants, and coordinates in the air and substrate regions.

Elliptic polarization of the magnetic field makes quantitative field data especially pertinent for ferrite components and YIG resonators. Knowledge of the field is also useful in the design of slot-excited dielectric resonators and directional couplers between two slots or a slot and microstrip. Application of the field formulas is also used in deriving equivalent circuits for transitions between slot line and coaxial line.

The formulas in this correspondence apply also to *sandwich* slot line; that is, a slotted metal sheet sandwiched between two substrates [5], [8].

Manuscript received February 26, 1971; revised June 28, 1971. This work was performed for Stanford Research Institute as a part of their study program for the U. S. Army Electronics Command under Contracts DAAB07-68-C-0088 and DAAB07-70-C-0044.
The author is a consultant to Stanford Research Institute, Menlo Park, Calif.

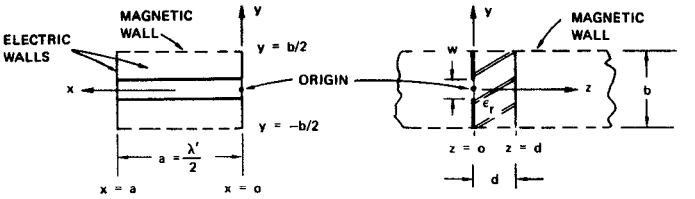

Fig. 1. Waveguide model used in field-distribution analysis.

II. Field Components

The configuration considered here is shown in Fig. 1. As in the earlier analysis [1], the slot-line problem is reduced to a rectangular waveguide problem by inserting electric walls in the planes perpendicular to the slot at $x=0$ and $x=a=\lambda'/2$, and magnetic walls at $y=\pm b/2$.

A pair of slot-line waves travel in the $+x$ and $-x$ direction with wavelength λ' substantially smaller than the free-space wavelength λ. For b sufficiently large (typically $b>\lambda'$), the fields at the magnetic walls are very small, and therefore b has negligible effect on the fields near the slot.

On the air side of the slot ($z\leq 0$), five field components exist: E_y, E_z, H_x, H_y, and H_z. On the substrate side these plus E_x exist. The coordinates x, y, z, the dimensions w, d, b, and the relative permittivity ϵ_r are all defined in Fig. 1. A factor $e^{j(\omega t-2\pi x/\lambda')}$ is assumed for each field component implying wave propagation in the $+x$ direction only. V_0 is the voltage directly across the slot.

The complete set of field-component formulas is contained in a

pair of reports [9], [10]. They were derived by summing the infinite set of TE and TM modes in the rectangular waveguide model. The E_y and H_x amplitudes of each of these modes were determined in an earlier analysis [1], and the other component amplitudes follow by application of Maxwell's equations. Formulas for H_x and H_z are given below without derivation.

Air Side of Slot, $z \leq 0$

$$H_x = -\frac{j2V_0}{\eta b}\left(\frac{\lambda}{\lambda'}\right)^2 \frac{b}{\lambda} \sum_{n=1/2,3/2\ldots} \left[\frac{1-(\lambda'/\lambda)^2}{nF_n}\right] \cdot \frac{\sin \pi n\delta}{\pi n\delta} \cdot \cos\frac{2\pi n y}{b} \cdot e^{-\gamma_n |z|} \tag{1}$$

$$H_z = \frac{2V_0}{\eta b} \cdot \frac{\lambda}{\lambda'} \sum_{n=1/2,3/2\ldots} \frac{\sin \pi n\delta}{\pi n\delta} \cos\frac{2\pi n y}{b} e^{-\gamma_n |z|}. \tag{2}$$

Substrate Side of Slot, $0 \leq x \leq d$

$$H_x = \frac{j2V_0}{\eta b}\left(\frac{\lambda}{\lambda'}\right)^2 \frac{b}{\lambda} \sum_{n=1/2,3/2\ldots} \frac{1}{nF_{n1}} \cdot \frac{\sin \pi n\delta}{\pi n\delta} \cdot \cos\frac{2\pi n y}{b} \cdot \left\{\left[\frac{F_{n1}^2 \coth q_n - \epsilon_r(\lambda'/\lambda)^2 \tanh r_n}{1+(b/n\lambda')^2}\right] \cosh \gamma_{n1} z - [1-\epsilon_r(\lambda'/\lambda)^2] \sinh \gamma_{n1} z\right\} \tag{3}$$

$$H_z = \frac{2V_0}{\eta b} \cdot \frac{\lambda}{\lambda'} \sum_{n=1/2,3/2\ldots} \frac{\sin \pi n\delta}{\pi n\delta} \cdot \cos\frac{2\pi n y}{b} \cdot [\cosh \gamma_{n1} z - \coth q_n \sinh \gamma_{n1} z]. \tag{4}$$

Substrate Side of Slot, $z \geq d$

$$H_x = \frac{j2V_0}{\eta b}\left(\frac{\lambda}{\lambda'}\right)^2 \frac{b}{\lambda} \sum_{n=1/2,3/2\ldots} \frac{\sin \pi n\delta}{\pi n\delta} \cdot \cos\frac{2\pi n y}{b} \cdot \left\{\left[\frac{F_{n1}^2 \coth q_n - \epsilon_r(\lambda'/\lambda)^2 \tanh r_n}{1+(b/n\lambda')^2}\right] \cosh \gamma_{n1} d - [1-\epsilon_r(\lambda'/\lambda)^2] \sinh \gamma_{n1} d\right\} \frac{e^{-\gamma_n (z-d)}}{nF_{n1}} \tag{5}$$

$$H_z = \frac{2V_0}{\eta b} \cdot \frac{\lambda}{\lambda'} \sum_{n=1/2,3/2\ldots} \frac{\sin \pi n\delta}{\pi n\delta} \cos\frac{2\pi n y}{b} \cdot [\cosh \gamma_{n1} d - \coth q_n \sinh \gamma_{n1} d] e^{-\gamma_n (z-d)}. \tag{6}$$

In (1)–(6), $\eta = 376.7\ \Omega$ and $\delta = w/d$. The symbols F_n, F_{n1}, u, v, etc., are defined in an earlier paper [1].

These field formulas are derived assuming that the electric field E in the slot plane has only an E_y component, and E_y is constant across the slot. (E_y actually rises sharply to infinity at the zero-thickness electric-wall edges.) As a result of these asumptions, the formulas are approximate near the slot. At a distance of about a slot width from the slot's center, the error becomes negligible.

The infinite series in the above formulas converge very slowly near $y = z = 0$, and hence an electronic computer is essential. The following criterion for terminating the series at n_t has proved useful: $n_t = n_0/(1+z/z_1)$, where n_0 and z_1 are constants. In one typical case, $n_0 = 1000$, and $z_1 = 0.005$ in were appropriate. Hence 1000 terms were used at $z = 0$, and 10 terms at $z = 0.5$ in.

III. Comparison to Previous Hankel-Function Solution

In an earlier paper [1], closed-form expressions for the magnetic field on the air side of the slot line were derived for $w \to 0$. After suitable modifications, these formulas are

$$H_x = j\frac{\pi V_0}{\eta\lambda}\left[\left(\frac{\lambda}{\lambda'}\right)^2 - 1\right][jH_0^{(1)}(k_c r)] \tag{7}$$

$$H_r = \frac{\pi V_0}{\eta\lambda'} \sqrt{\left(\frac{\lambda}{\lambda'}\right)^2 - 1}\,[-H_1^{(1)}(k_c r)] \tag{8}$$

$$k_c = \frac{j2\pi}{\lambda} \sqrt{\left(\frac{\lambda}{\lambda'}\right)^2 - 1} \tag{9}$$

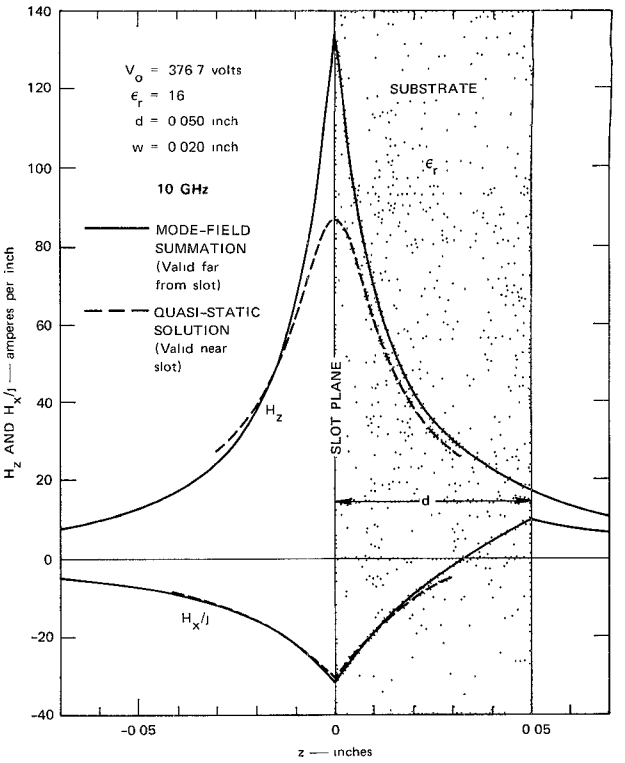

Fig. 2. Comparison of two solutions for H_z and H_x/j plotted along z axis.

where x is the direction of propagation (see Fig. 1) and $r = \sqrt{y^2+z^2}$ is the radial distance from the slot. The Hankel-function quantities $jH_0^{(1)}(j|x|)$ and $-H_1^{(1)}(j|x|)$ are real and positive, and are available in tables.

Equation (1) for H_x should be equivalent to (7) when $\delta = w/b$ is reduced to zero. Also, (2) for H_z should be equivalent to (8) along the z axis. (To apply (1) in the $z \geq 0$ region instead of $z \leq 0$, it is necessary to change the sign of H_x. Thus H_x/j and H_z are positive.) Despite their vast mathematical differences the two sets of formulas have been found to yield virtually identical values [9].

IV. Field Plots for Typical Cases

Equations (1)–(6) for H_x and H_z are plotted as solid lines versus z in Fig. 2. Slot-line parameters are $\epsilon_r = 16$, $d = 0.050$ in, and $w = 0.020$ in. The sharp-slope discontinuity in H_z at $z = 0$ cannot physically occur, and results from analysis approximations as discussed above. Error in the computed field components is moderate at about $z = \pm w/2$, and is very small at z beyond $\pm w$. Slope discontinuities in H_x at the substrate surfaces are correct behavior; they are caused by the discontinuous changes of ϵ_r versus z.

Improvement of the mode-summation analysis to eliminate error at z near 0 would require a large increase in computational complexity. A simpler approach is to derive field formulas accurate only near the slot, and to use these in correcting the field curves near $z = 0$. This approach uses the static E field derived by conformal mapping in the space surrounding an infinitely large zero-thickness slotted sheet [11]. The static E_y component is

$$E_y = \frac{2V_0}{\pi w}\left[1 - \left(\frac{2y}{w}\right)^2\right]^{-1/2}, \quad \text{on the } y \text{ axis} \tag{10}$$

and

$$E_y = \frac{2V_0}{\pi w}\left[1 + \left(\frac{2z}{w}\right)^2\right]^{-1/2}, \quad \text{on the } z \text{ axis.} \tag{11}$$

These are exact when b and d are infinite and the frequency is zero. If a uniform ϵ_r' exists throughout space on both sides of the slotted

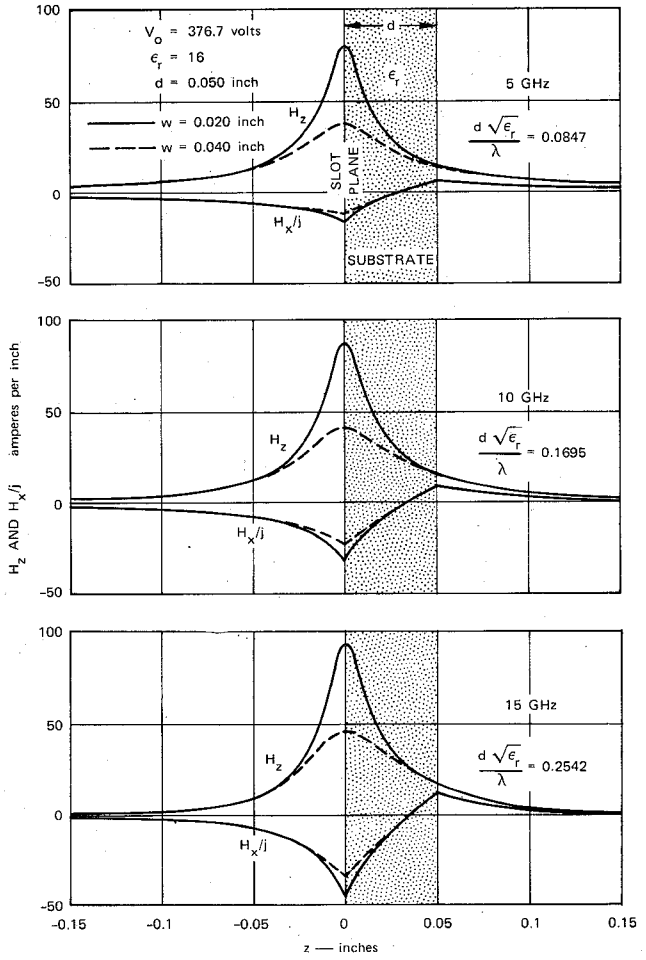

Fig. 3. Graphs of H_z and H_x/j along z axis for several slot widths and frequencies.

sheet, a TEM wave will propagate with $H_z=\sqrt{\epsilon_r'}E_y/\eta$. A comparison of the mode-summation equations for E_y and H_z on the air side of the slot yields $H_z=(\lambda/\lambda')E_y/\eta$, while a comparison for the substrate side yields the same relation when z is near zero (or for all z, if $d=\infty$). Therefore, we are justified in using the following quasi-static formula

$$H_z=\frac{\sqrt{\epsilon_r'}}{\eta}E_y, \qquad \epsilon_r'=\left(\frac{\lambda}{\lambda'}\right) \tag{12}$$

to compute H_z close to the slot.

Quasi-static H_z is plotted as a dotted curve in Fig. 2, and lies in a reasonable relationship to the solid curve. The two curves can clearly be blended together by transitions to yield a single curve of good accuracy. This was done in the field graphs in Fig. 3.

Application of Maxwell's equation $\nabla\times\boldsymbol{H}=j\omega\epsilon\boldsymbol{E}$ yields

$$H_x=H_x(z_1)-\frac{j2\pi}{\lambda'}\left[1-\epsilon_r\left(\frac{\lambda'}{\lambda}\right)^2\right]\int_{z_1}^{z}H_z\,dz. \tag{13}$$

To compute H_x versus z, the best choice of z_1 is at a point in the air region $z\leq 0$ where both the mode-summation and quasi-static solutions for H_z have good accuracy. In Fig. 2, $z_1=-0.016$ in is a suitable choice. The interval along the z axis, from $z=z_1$ to $z=0.010$ in is a region of good accuracy for the quasi-static solution. Substitution of (11) and (12) in (13) gives the following for H_x versus z with $y=0$:

$$H_x=H_x(z_1)-\frac{j2V_0}{\lambda\eta}\left[\left(\frac{\lambda}{\lambda'}\right)^2-\epsilon_r\right]\cdot\left[\sinh^{-1}\left(\frac{2z}{w}\right)-\sinh^{-1}\left(\frac{2z_1}{w}\right)\right]. \tag{14}$$

In using (14), evaluate $H_x(z_1)$ from the mode-summation formula (1). At $z\leq 0$, let $\epsilon_r=1$; at $z\geq 0$, let ϵ_r equal the substrate value. Equation (14) for H_x is plotted as a dotted curve in Fig. 2. Blending the solid and dotted curves to obtain a corrected curve is a simple matter.

Fig. 3 shows computed curves of H_z and H_x/j versus z for $y=0$, $V_0=376.7$ V, $\epsilon_r=16$, $d=0.050$ in, $w=0.020$ and 0.040 in, and $f=5$, 10, and 15 GHz. The mode-summation formulas were modified near $z=0$ by the quasi-static formulas, as described in the preceding paragraphs. Above 15 GHz, $d\sqrt{\epsilon_r}/\lambda>0.25$ and interference from surface waves is possible. Because H_z is real and H_x imaginary, the magnetic field is elliptically polarized in the z and x plane. The axial ratio is $\overline{AR}=|H_z/H_x|$. Note that $|H_z/H_x|$ is greater than one for all z values, and hence the condition $\overline{AR}=1$ for circular polarization is not met at any point. The curves show that the closest approach to circular polarization occurs at the largest w and the highest f. For example, with $w=0.040$ in and $f=15$ GHz, $\overline{AR}=1.351$ and 1.472 at the $z=0$ and $z=d$ surfaces of the substrate, respectively. Between $z=0$ and $z=d$ in the substrate, $\overline{AR}$ rises and is infinite at about $z=0.7d$. The point $\overline{AR}=\infty$ occurs where H_z/j passes through zero. Since the sign of H_z/j changes at this point, the direction of rotation of the elliptical polarization vector also changes.

References

[1] S. B. Cohn, "Slot line on a dielectric substrate," *IEEE Trans. Microwave Theory Tech.*, vol. MTT-17, pp. 768–778, Oct. 1969.
[2] E. A. Mariani, C. P. Heinzman, J. P. Agrios, and S. B. Cohn, "Slot line characteristics," *IEEE Trans. Microwave Theory Tech.*, vol. MTT-17, pp. 1091–1096, Dec. 1969.
[3] G. H. Robinson and J. L. Allen, "Slot line application to miniature ferrite devices," *IEEE Trans. Microwave Theory Tech.*, vol. MTT-17, pp. 1097–1101, Dec. 1969.
[4] F. C. de Ronde, "A new class of microstrip directional couplers," in *1970 G-MTT Symp. Dig.*, pp. 184–189, 1970.
[5] E. A. Mariani and J. P. Agrios, "Slot line filters," in *1970 G-MTT Symp. Dig.*, pp. 190–195, 1970.
[6] J. K. Hunton and J. S. Takeuchi, "Recent developments in microwave slot line mixers and frequency multipliers," in *1970 G-MTT Symp. Dig.*, pp. 196–199, 1970.
[7] H. J. Schmitt, "Fundamentals of microwave integrated circuits," in *Proc. Swedish Seminar on New Microwave Components* (Stockholm, Sweden), 1970.
[8] S. B. Cohn, "Sandwich slot line," *IEEE Trans. Microwave Theory Tech.* (Corresp.), vol. MTT-19, pp. 773–774, Sept. 1971.
[9] E. G. Cristal, R. Y. C. Ho, D. K. Adams, S. B. Cohn, L. A. Robinson, and L. Young, "Microwave synthesis techniques," Stanford Res. Inst., Menlo Park, Calif., Contract DAAB07-68-C-0088, SRI Project 6884, Final Rep., Nov. 1969.
[10] D. Chambers, S. B. Cohn, E. G. Cristal, and L. Young, "Microwave active network synthesis," Stanford Res. Inst., Menlo Park, Calif., Contract DAAB07-70-C-004, SRI Project 8245, Semiannu. Rep., June 1970.
[11] E. Weber, "Mapping of fields," in *Electromagnetic Fields*, vol. I. New York: Wiley, 1950, p. 340, eq. (38); also p. 304, eq. (7).

A Highly Stabilized K_a-Band Gunn Oscillator

S. NAGANO AND S. OHNAKA

***Abstract*—The construction and experimental results of a highly stabilized K_a-band Gunn oscillator are described. The frequency stability is 3×10^{-5} at 25 GHz over the temperature range from 0 to 50°C. An output power of more than 20 mW has been obtained in the frequency range up to 30 GHz. The frequency-saturation effect is also described.**

The Gunn diode is one of the most promising devices for local oscillator applications in microwave and millimeterwave communication receivers because of their low AM noise. However, the FM noise or the short-term stability is larger than that of a reflex klystron, and the long-term stability is also worse. The frequency stability of the ordinary Gunn oscillators and the required value of the stability in the communication systems are in the order of 10^{-3} and 10^{-5}, respectively, over the temperature range from 0 to 50°C. The stability can be improved by increasing the stored energy in the oscillator cavity without any sacrifice of the output power. This can be achieved

Manuscript received March 18, 1971; revised May 19, 1971.
The authors are with the Nippon Electric Company, Central Research Laboratories, Kawasaki, Japan.